ACS APPLIED MATERIALS & INTERFACES

Research Article

www.acsami.org

# Compact, Programmable, and Stable Biofunctionalized Upconversion Nanoparticles Prepared through Peptide-Mediated Phase Transfer for High-Sensitive Protease Sensing and *in Vivo* Apoptosis Imaging

Tao Zeng,[†] Tao Zhang,[†] Wei Wei,[†] Zhi Li,[†] Dan Wu,[†] Li Wang,[†] Jun Guo,[‡] Xuewen He,[†] and Nan Ma*[,†]

[†]Key Laboratory of Health Chemistry and Molecular Diagnosis of Suzhou, College of Chemistry, Chemical Engineering and Materials Science, and [‡]Testing and Analysis Center, Soochow University, Suzhou, Jiangsu 215123, People's Republic of China

Supporting Information

**ABSTRACT:** Protease represents an important class of biomarkers for disease diagnostics and drug screening. Conventional fluorescence-based probes for *in vivo* protease imaging suffer from short excitation wavelengths and poor photostability. Upconversion nanoparticles (UCNPs) hold great promise for biosensing and bioimaging because of their deep-tissue excitability, robust photostability, and minimal imaging background. However, producing highly stable and compact biofunctionalized UCNP probes with optimal bioresponsivity for *in vivo* imaging of protease activities still remains challenging and has not been previously demonstrated. Herein, we report facile preparation of highly compact and stable biofunctionalized UCNPs through peptide-mediated phase transfer for high-sensitive detection of protease *in vitro* and *in vivo*. We demonstrate that the polyhistidine-containing chimeric peptides could displace oleic acid molecules capped on UCNPs synthesized in organic solvents and, thereby, directly transfer UCNPs from the chloroform phase to the water phase. The resulting UCNPs possess high stability, programmable surface properties, and a compact coating layer with minimized thickness for efficient luminescence resonance energy transfer (LRET). On the basis of this strategy, we prepared LRET-based UCNP probes with optimal bioresponsivity for *in vitro* high-sensitive detection of trypsin and *in vivo* imaging of apoptosis for chemotherapy efficacy evaluation. The reported strategy could be extended to construct a variety of peptide-functionalized UCNPs for various biomedical applications.

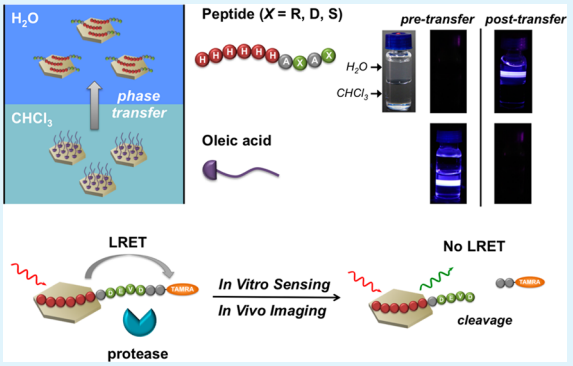


**KEYWORDS:** *upconversion nanoparticle, phase transfer, peptide, protease, in vivo imaging, biosensing*

## INTRODUCTION

Protease plays critical roles in many biological and physiological processes. Developing novel techniques for high-sensitive detection and imaging of protease activities would provide a valuable means for disease diagnostics, drug screening, and investigation of protease functions during disease development and treatment.[1] The proteolysis activities of protease have been harnessed to devise a variety of techniques for the detection of protease *in vitro*,[2−6] whereas imaging of protease activities *in vivo* remains much more challenging and relatively less accomplished. Conventional fluorescence-based imaging probes are limited by their short excitation wavelength and poor photostability, which would deteriorate both imaging depth and sensitivity. Developing novel universal platforms for high-sensitive *in vivo* protease sensing is still in urgent need.

Lanthanide-doped upconversion nanoparticles (UCNPs),[7] which could convert two or more low-energy near-infrared (NIR) photons into a high-energy photon through a nonlinear anti-Stokes process,[8] have emerged as an important class of imaging contrast agents with deep-tissue excitability, robust photostability, low toxicity, and minimal autofluorescence background.[9] However, producing highly stable and compact biofunctionalized UCNP probes with optimal bioresponsivity for *in vivo* imaging of protease activities still remains challenging and has not been previously demonstrated. Because high-quality UCNPs are mostly synthesized in organic solvents, subsequent solubilization and biofunctionalization are crucial to obtain bioactive UCNPs for biosensing and bioimaging applications.[10] To this end, different strategies have been developed to solubilize UCNPs in aqueous solution, including ligand exchange,[11] silanization,[12] ligand oxidization,[13] and layer-by layer assembly, and then further attach biomolecules to the nanoparticle surface through bioconjugation.[14−16] In addition to their complexity, most exsiting strategies add a relatively thick layer on the UCNPs that would create a barrier for efficient energy transfer between UCNP donors and surrounding acceptors for sensing applications. To obtain luminescence resonance energy transfer (LRET)-based UCNP probes with

Received: February 13, 2015
Accepted: May 13, 2015
Published: May 13, 2015





DOI: 10.1021/acsami.5b01446
ACS Appl. Mater. Interfaces 2015, 7, 11849−11856

high bioresponsivity, it is imperative to construct highly compact and stable biofunctionalized UCNPs, which still remains difficult to achieve via conventional methods.

Peptides are naturally occurring biopolymers and have been widely used for enzyme sensing,[17] biotargeting,[18] and drug delivery.[19] They are readily available via solid-phase synthesis and are highly programmable by incorporating different amino acid building blocks into the peptides. Polyhistidine-containing peptides are known to chelate $Ni^{2+}$ ions for protein purification.[20] This metal-chelating property was further applied to biofunctionalization of quantum dots (QDs), where the polyhistidine peptide could bind with heavy metal ions displayed on QDs.[21] However, despite the drastic increasing research interests on UCNPs in recent years, peptide-mediated direct solubilization and biofunctionalization of UCNPs have not been demonstrated to date. In particular, because the host compositions of UCNPs (e.g., $NaYF_4$) are distinct from all of the semiconductor and metal nanoparticles,[22] it remains unknown whether the metal-chelating peptides could directly bind to the UCNP surface.

Herein, we report a new general facile strategy for the preparation of highly compact and stable biofunctionalized UCNPs through peptide-mediated phase transfer for high-sensitive detection of protease activities *in vitro* and *in vivo*. We designed a series of chimeric peptides containing a polyhistidine domain (HHHHHH) for UCNP binding and a bioactive domain for biomolecule sensing. We discover that the chimeric peptides could displace oleic acid (OA) molecules capped on the original UCNPs and, thereby, directly extract UCNPs from the chloroform phase to the water phase (Figure 1a). This facile phase transfer process would allow us to conveniently functionalize UCNPs with various peptide sequences and, thus, could serve as a general strategy for the preparation of peptide-functionalized UCNPs. The resulting UCNPs possess high stability, programmable surface properties, and a compact coating layer with minimized thickness for efficient LRET. On the basis of their superior properties, the as-prepared peptide−UCNP probes were further applied to the detection of trypsin activities with sensitivity 1 order of magnitude higher than other methods. More importantly, we for the first time demonstrate *in vivo* imaging of caspase-3 activity using these UCNP probes, which exhibits high specificity and could be used to monitor chemotherapy efficacy for cancer treatment.

## EXPERIMENTAL SECTION

**Chemicals.** $YCl_3{\cdot}6H_2O$ (99.99%), $YbCl_3{\cdot}6H_2O$ (99.9%), $TmCl_3$ (99.9%), $ErCl_3{\cdot}6H_2O$ (99.9%), NaOH (98%), $NH_4F$ (98%), OA (90%), 1-octadecene (ODE, 90%), trypsin, and bovine serum albumin (BSA 98%) were purchased from Sigma-Aldrich. Dulbecco's modified Eagle's medium (DMEM), RPMI-1640 medium, fetal bovine serum (FBS), trypsin−ethylenediaminetetraacetic acid (EDTA) (0.25%), and phosphate-buffered saline (PBS) were purchased from Hyclone. Doxorubicin (DOX) was purchased from Melone Pharmaceutical Co., Ltd. All of other chemicals are analytical-grade and used without further purification.

The following peptides were synthesized and purified by ChinaPeptides Co., Ltd. (left, N terminus; right, C terminus; $-NH_2$ indicates C-terminal amidation): HHHHHHARAR−$NH_2$, HHHHHHADAD−$NH_2$, HHHHHHASAS−$NH_2$, DDDDDDADAD−$NH_2$, and ADAD−$NH_2$. TAMRA-labeled peptides: HHHHHHYGKAGK−TAMRA and HHHHHHGDEVDAK−TAMRA.

**Synthesis of OA-Capped UCNPs.** $\beta$-$NaYF_4$:20% Yb, 2% Er and $\beta$-$NaYF_4$:25% Yb, 0.5% Tm upconversion nanoparticles were synthesized using a solvothermal method described previously.[7,23]

Briefly, 5 mL of methanol solution of $LnCl_3$ (1.0 mmol, Ln = Y, Yb, and Tm/Er) was mixed with 6 mL of OA and 15 mL of ODE in a three-neck round-bottom flask. The resulting mixture was heated at 150 °C under argon flow for 30 min to form a clear light yellow solution. After cooling to 50 °C, 10 mL of methanol solution containing 0.1480 g of $NH_4F$ and 0.10 g of NaOH was added and the solution was vigorously stirred for 30 min. Then, the slurry was slowly heated and kept at 110 °C for 10 min to remove methanol. Next, the reaction mixture was protected with an argon atmosphere, quickly heated to 310 °C (about 15 °C $min^{-1}$), and maintained for 1.5 h. The products were isolated by adding ethanol and centrifuged without size-selective fractionation. The final $NaYF_4$:20% Yb, 2% Er or $NaYF_4$:25% Yb, 0.5% Tm nanocrystals were redispersed in chloroform with a 5 mg $mL^{-1}$ concentration after washing with chloroform/ethanol (1:1) 3 times.

**Peptide-Mediated Phase Transfer of UCNPs.** A total of 300 $\mu$L of OA-capped UCNPs (5 mg/mL) and 300 $\mu$L of peptide in $H_2O$ (various peptide concentrations) were added to a glass vial and then vigorously stirred for 6−8 h. Afterward, the UCNPs were efficiently transferred to the top water layer from the chloroform layer. The UCNP solution (top layer) was then collected and stored at 4 °C for further use.

**Transmission Electron Microscopy (TEM) Characterization.** Each UCNP sample (2.5 mg/mL) was dispersed onto a 3 mm copper grid covered with a continuous carbon film and dried at room temperature. For peptide staining, 2% phosphotungstic acid was added to the sample and incubated for 10 min. Subsequently, phosphotungstic acid solution was removed from the grid, and the sample was rinsed with distilled water. TEM was performed using a Tecnai $G^2$ 20 (FEI, Hillsboro, OR) transmission electron microscope operating at 185 kV.

**Atomic Force Microscopy (AFM) Characterization.** OA-capped UCNP solution (0.5 mg/mL) was dropped onto fleshly prepared mica and dried at room temperature. The UCNPs were imaged with AFM (Bruker Multi-Mode 8) under ScanAsyst-Air mode using a ScanAsyst-Air probe (Bruker).

**Optical Characterization.** The photoluminescence spectra were recorded using a fiber fluorescence spectrophotometer (AvaSpec-2048) equipped with a 980 nm laser (1 W, Shanghai Dream Lasers Technology Co., Ltd., power density of 6.6 W/$cm^2$) as the excitation light source. The integration time was set to 100 ms. The absorption spectra were recorded using a UV−vis spectrophotometer (Agilent 8453).

**Dynamic Light Scattering (DLS) and $\zeta$ Potential.** Hydrodynamic sizes and $\zeta$ potential of UCNPs were measured on a Zetasizer Nano ZS90 (Malvern).

**Peptide-Coated UCNPs for Trypsin Detection.** *Preparation of Peptide−TAMRA-Coated UCNPs.* A total of 500 $\mu$L of OA-capped UCNPs (5 mg/mL) in chloroform and 500 $\mu$L of $(H)_6$YGKAGK−TAMRA (150 $\mu$M) in $H_2O$ were added to a glass vial and then vigorously stirred for 8 h. Afterward, the UCNPs were efficiently transferred to the upper water layer from the chloroform layer. The UCNP solution was transferred to a microtube. After sonication for 3 min, peptide-coated UCNPs were centrifuged at 4500 rpm for 10 min to remove excess peptides in the supernatant and resuspended in 500 $\mu$L of Tris buffer (50 mM, pH 8.2) containing 150 $\mu$M $(H)_6$YGKAGK−TAMRA. The resulting UCNP solution was left at room temperature for 1 day, and the free peptides were removed, as described above. The purified nanoparticles were redispersed in Tris buffer (50 mM, pH 8.2) and stored at 4 °C for further use.

*Enzyme Cleavage and Control Experiments.* Trypsin stock solution (10 mg $mL^{-1}$) was prepared by dissolving trypsin powder in sterilized HCl (0.001 M, pH 3.0). BSA stock solution (50 mg $mL^{-1}$) was prepared by dissolving BSA powder in sterilized water. UCNP−$(H)_6$YGKAGK−TAMRA (115 $\mu$L, UCNP concentration = 5.0 mg $mL^{-1}$) and various amounts of trypsin (final trypsin concentration for the reaction = 0, 0.01, 0.05, 0.5, 1, 5, 10, 50, 100, 500, and 1000 nM) were added to Tris buffer (final concentration = 50 mM, pH 8.2) to a total volume of 200 $\mu$L. The enzyme cleavage reaction was conducted in a water bath at 37 °C for 2 h.[3] BSA with


DOI: 10.1021/acsami.5b01446
ACS Appl. Mater. Interfaces 2015, 7, 11849−11856

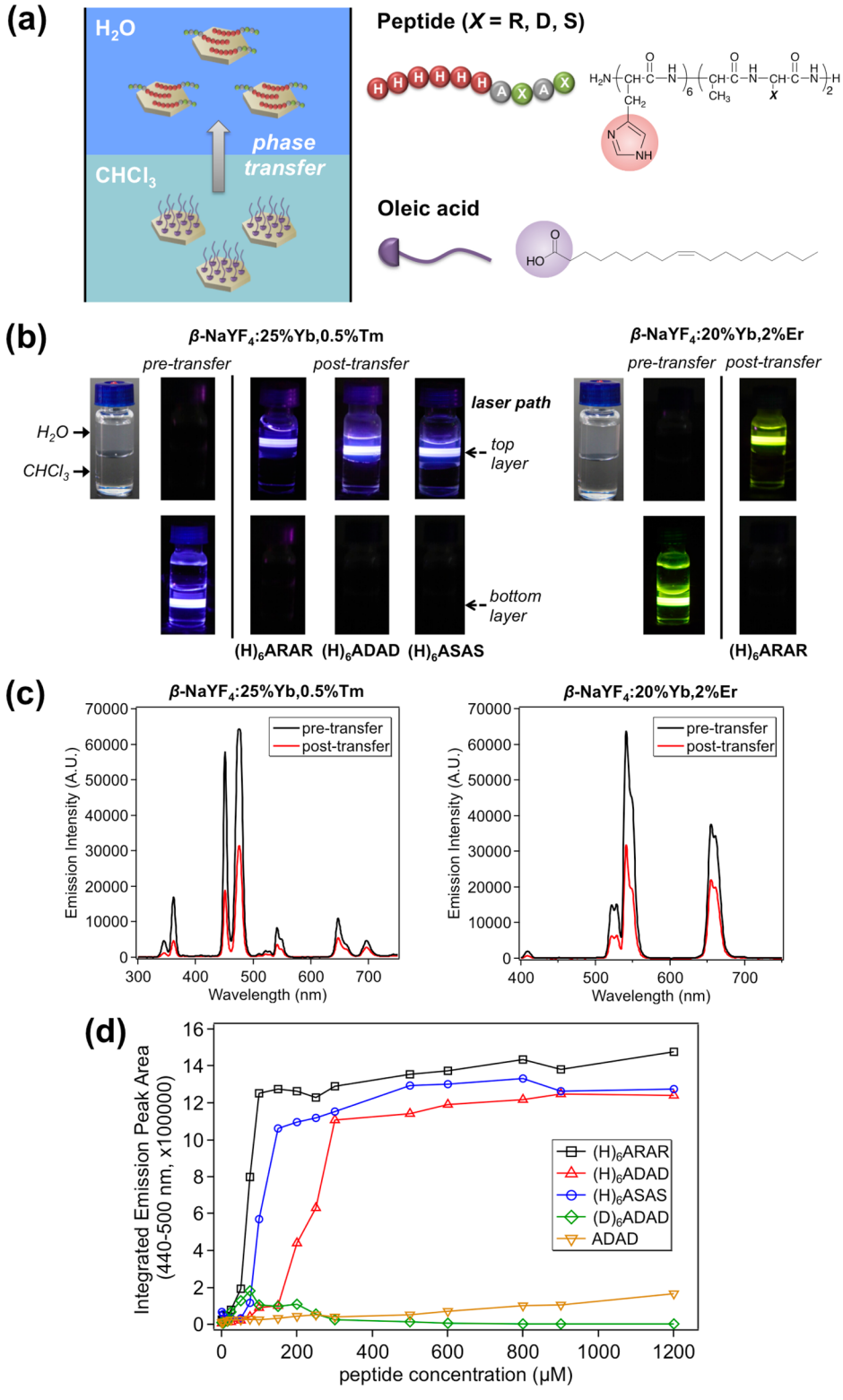


**Figure 1.** Peptide-mediated phase transfer for one-step preparation of biofunctionalized UCNPs. (a) Schematic illustration of the phase transfer process and chemical structures of polyhistidine-containing peptides and OA. (b) Bright-field and luminescence photographs of pre- and post-transferred $\beta$-$NaYF_4$:25% Yb, 0.5% Tm and $\beta$-$NaYF_4$:20% Yb, 2% Er UCNPs with various chimeric peptides. The top water layer and bottom chloroform layer are excited with a 980 nm laser to monitor the phase transfer process. (c) UCL spectra of pre- and post-transferred $\beta$-$NaYF_4$:25% Yb, 0.5% Tm and $\beta$-$NaYF_4$:20% Yb, 2% Er UCNPs. (d) Stability of $\beta$-$NaYF_4$:25% Yb, 0.5% Tm UCNPs transferred with various peptides at different peptide concentrations. The UCNPs were stored at room temperature for 48 h before measurements.

various concentrations (final BSA concentration for the reaction = 0, 1, 10, 100, $10^3$, $10^4$, and $10^5$ nM) was used as controls for the reaction.

**Cell Culturing and 3-(4,5-Dimethylthiazol-2-yl)-2,5-diphenyltetrazolium Bromide (MTT) Assay.** *Cell Culturing.* HeLa cells were cultured on 25 $cm^2$ cell culture plates with vent caps (Corning) in DMEM supplemented with 10% fetal bovine serum (FBS) and 1% pen/strep (100 units $mL^{-1}$ penicillin and 100 mg $mL^{-1}$ streptomycin) in a humidified incubator at 37 °C containing $CO_2$ (5%). KB cells



DOI: 10.1021/acsami.5b01446
ACS Appl. Mater. Interfaces 2015, 7, 11849−11856

were cultured on 25 $cm^2$ cell culture plates in RPMI-1640 medium supplemented with 10% FBS and 1% pen/strep (100 units $mL^{-1}$ penicillin and 100 mg $mL^{-1}$ streptomycin) in a humidified incubator at 37 °C containing $CO_2$ (5%). Cells that had been grown to subconfluence were dissociated from the surface with 0.25% trypsin−EDTA.

*MTT Assay.* $(H)_6$GDEVDAK−TAMRA-coated UCNPs were prepared as described above and resuspended in 1× PBS. Aliquots (100 μL) of HeLa and KB cells were seeded ($1.5 \times 10^4$ cells) into a 96 well plate (Costar). After overnight incubation, cell media were removed and the cells were washed 3 times with 1× PBS. Next, 100 μL of cell media containing 1, 5, 25, 50, 100, 250, and 500 μg $mL^{-1}$ $(H)_6$GDEVDAK−TAMRA-coated UCNPs were added to each well, and the cells were incubated at 37 °C for 24 h. After that, the media were replaced with 100 μL of cell media containing 5 mg $mL^{-1}$ MTT, and the cells were incubated at 37 °C for 4 h. Formazan crystals were dissolved in 150 μL of dimethyl sulfoxide (DMSO) with gentle agitation for 10 min. Cells treated with FBS-containing media alone and Triton X-100 were used as low- and high-cell death controls, respectively. The absorbance of the supernatant at 490 nm was measured using a TECAN Infinite M200 PRO plate reader.

**Chemotherapy Mouse Model.** Nude mice (4−6 weeks) were purchased from Soochow University Laboratory Animal Center. The $1 \times 10^6$ KB cells in 100 μL of RPMI-1640 medium were subcutaneously inoculated in each nude mouse. As the tumor volumes approached 40 $mm^3$ (approximately 15−20 days), the tumors were treated with doxorubicin (DOX) (4 mg of DOX/kg of mouse body weight) or saline through intratumoral injection. After 4 days, the same tumors were treated with DOX and saline for the second time. Tumors were sized in two dimensions using a vernier caliper, and the tumor volume in cubic millimeters was approximated by the formula $V(\text{tumor}) = (\text{width})^2 \times \text{length}/2$.

***In Vivo* Apoptosis Imaging.** $(H)_6$GDEVDAK−TAMRA-coated UCNPs were prepared as described above and resuspended in 1× PBS. At 2 days after the second DOX treatment, 40 μL of $(H)_6$GDEVDAK−TAMRA-coated UCNPs (5 mg $mL^{-1}$ UCNPs) was intratumorally injected into the tumor and the upconversion luminescence (UCL) imaging was performed on a Maestro In-Vivo Imaging System (Caliper Life Science) equipped with a 980 nm laser (power density = 0.3 W $cm^{-2}$) and a 850 nm short pass emission filter (Chroma). The UCL signal was collected between 450 and 600 nm. The green emission intensity of each tumor was quantified using ImageJ software.

## RESULTS AND DISCUSSION

To demonstrate peptide-mediated phase transfer, we synthesized two popular types of UCNPs, β-$NaYF_4$:25% Yb, 0.5% Tm and β-$NaYF_4$:20% Yb, 2% Er, using a conventional solvothermal method.[7,23] These UCNPs were purified and dispersed in chloroform for phase transfer. The Tm- and Er-doped UCNPs emit strong luminescence with visible blue and green color, respectively, when excited with 980 nm laser (Figure 1b). Phase transfer was conducted at room temperature by mixing peptides in water and UCNPs in chloroform under vigorous stirring. To show the versatility of this approach, we tested three chimeric peptides with different net charges [$(H)_6$ARAR (+2), $(H)_6$ASAS (0), and $(H)_6$ADAD (−2)]. As shown in Figure 1b, all three peptides could successfully transfer Tm-doped UCNPs from the bottom chloroform layer to the top water layer after 6−8 h. This phase transfer process is highly efficient without residual luminescence in the chloroform layer. Most importantly, the UCNPs in water are still highly luminescent and well-dispersed. The upconversion luminescence (UCL) spectra of UCNPs in water possess characteristic emission peaks that are identical to the original UCNPs in chloroform. About 50% luminescence intensity was retained after phase transfer (Figure 1c). The stabilities of the resulting UCNPs are dependent upon the peptide concentrations for phase transfer. UCNPs transferred under low peptide concentrations tend to aggregate after prolonged storage, and higher peptide concentrations (depending upon the net charge of the peptide) are necessary to obtain stable UCNPs in aqueous solution (Figure 1d and Figure S1 of the Supporting Information). To elucidate the role of polyhistidine in phase transfer and UCNP stabilization, a peptide without polyhistidine (ADAD) and a peptide with a polyaspartic acid domain [$(D)_6$ADAD] were used for phase transfer. In this case, no stable UCNPs could be obtained in aqueous solution even at high peptide concentrations (Figure 1d). Although these two peptides could extract UCNPs from the chloroform layer, they are not competent to stabilize UCNPs in water but lead to the formation of large aggregates (see Figure S2 of the Supporting Information). Similar phase transfer results were observed for Er-doped UCNPs (Figure 1b). ζ potentials of each peptide-capped UCNPs are in accordance with the net charges of the corresponding chimeric peptides used for phase transfer (Table 1). DLS measurements

**Table 1. ζ Potentials and Average Hydrodynamic Sizes of OA- and Peptide-Capped β-$NaYF_4$:25% Yb, 0.5% Tm UCNPs (600 μM Peptides)**

| ligand | ζ potential (mV) | average HD size (nm) |
|---|---|---|
| OA | | 64.8 |
| $(H)_6$ARAR | +44.0 | 89.9 |
| $(H)_6$ADAD | −39.6 | 86.4 |
| $(H)_6$ASAS | +0.02 | 88.6 |
| ADAD | | 925 (aggr.) |
| $(D)_6$ADAD | | 1352 (aggr.) |

show that the as-prepared peptide−UCNPs are highly monodispersed (Table 1 and Figure 2). The average hydrodynamic sizes of the UCNPs increased by ∼20−25 nm (600 μM peptides) and ∼8 nm (100 μM peptides) after phase transfer (Figure 2), indicating effective surface modification of the UCNPs. These UCNPs were further characterized by TEM. Monodisperse hexagonal-phase $NaYF_4$:25% Yb, 0.5% Tm in chloroform could be visualized in TEM images (Figure 3). After phase transfer, the UCNPs maintained their morphology and monodispersity. A uniform low contrast layer on UCNPs could be visualized in high-resolution TEM images (Figure 3), which corresponds to the peptides capped on the UCNP surface. A staining TEM image further confirms the presence of the peptide layer on the UCNP surface (see Figure S3 of the Supporting Information). It is noteworthy that the thickness of this layer would increase with a higher peptide concentration (Figure 3). The as-prepared peptide-capped UCNPs exhibit extremely high stability at various pH values, high ionic strength, and different buffer solutions (see Figure S4 of the Supporting Information).

Next, we applied this strategy to prepare peptide-capped UCNPs for protease sensing. In comparison to conventional fluorophores, NIR excitation of UCNPs would avoid sample autofluorescence and the exceptional narrow emission peaks of UCNPs are ideal for energy-transfer-based biosensing. As a proof-of-concept experiment, we used β-$NaYF_4$:20% Yb, 2% Er UCNPs to construct a LRET-based probe to detect trypsin, an important serine protease that is involved in cancer development.[24] Er-doped UCNPs contain two major emission peaks at 540 and 655 nm that are attributed to $^4S_{3/2}$ to $^4I_{15/2}$ and $^4F_{9/2}$ to $^4I_{15/2}$ transitions, respectively.[25] We choose TAMRA as energy acceptors to selectively quench the green emission peak,


DOI: 10.1021/acsami.5b01446
ACS Appl. Mater. Interfaces 2015, 7, 11849−11856

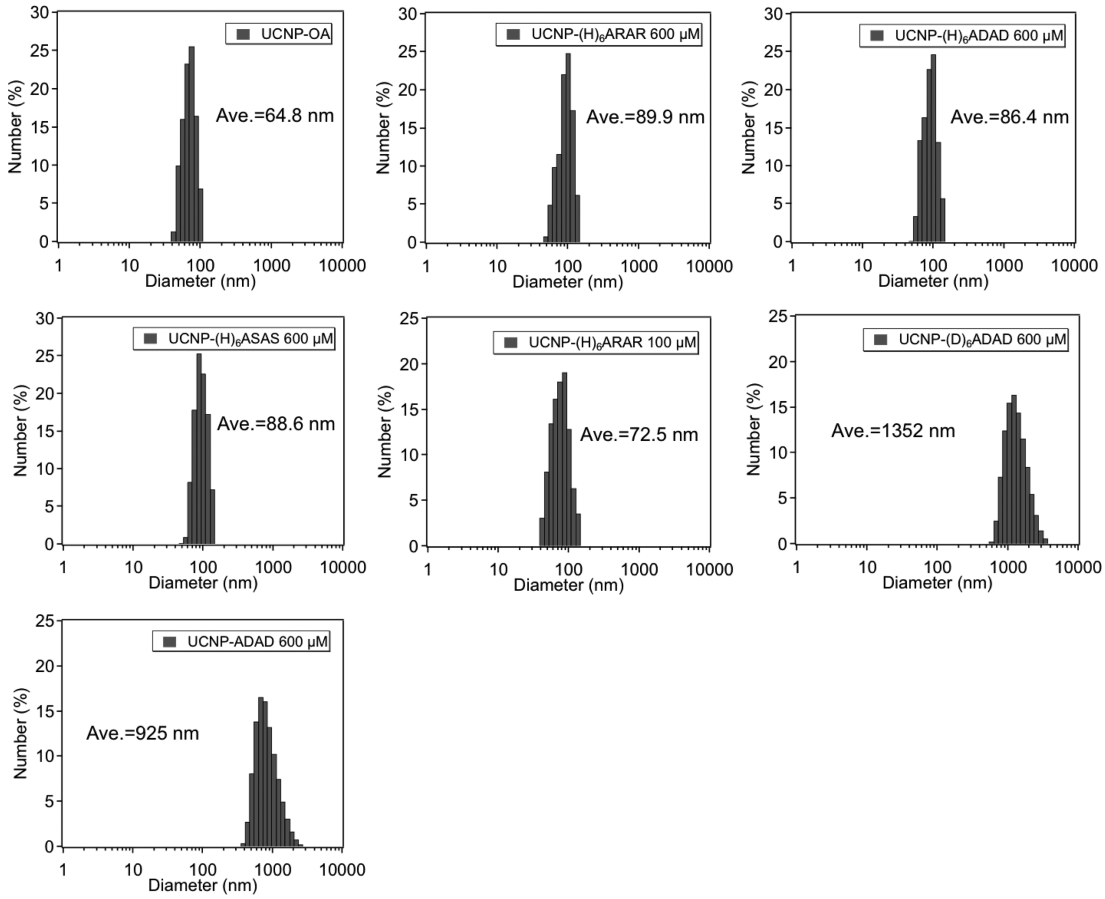


**Figure 2.** Hydrodynamic size of OA- and peptide-capped $\beta$-$NaYF_4$:25% Yb, 0.5% Tm UCNPs (600 and 100 $\mu$M peptides).

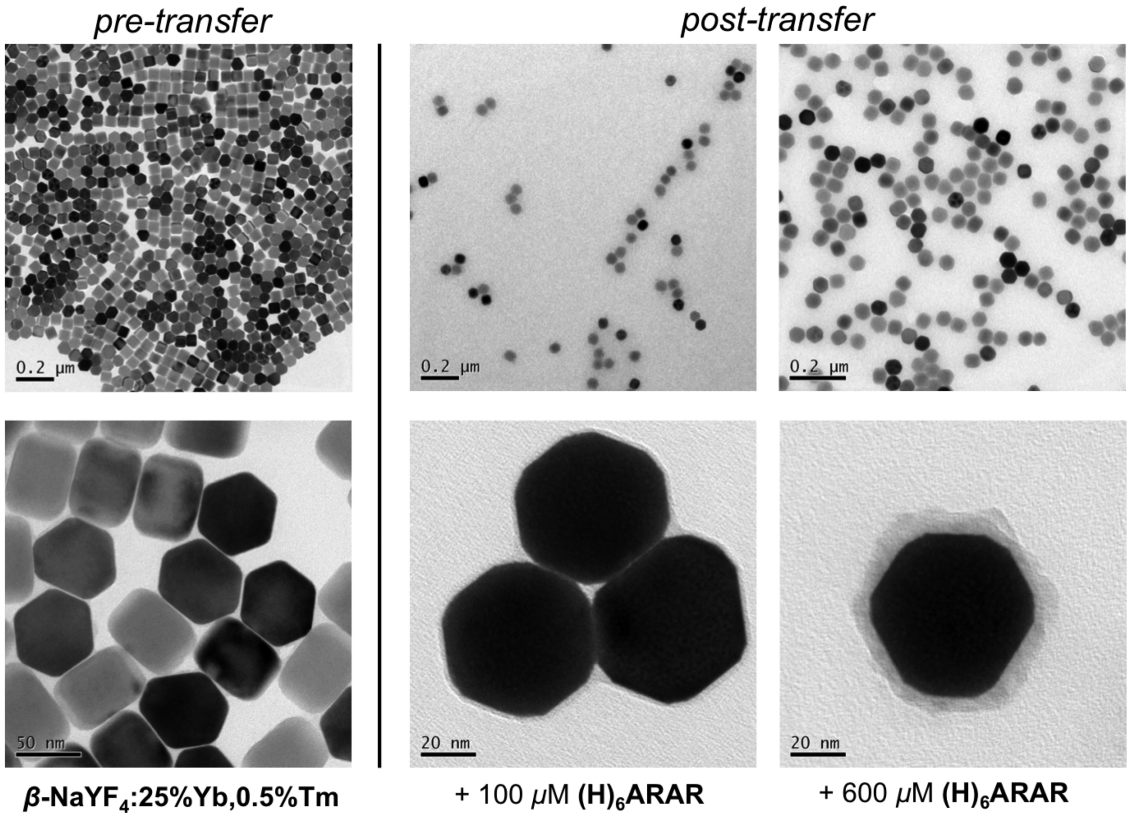


**Figure 3.** Low-magnification (upper panel) and high-magnification (lower panel) TEM images of pre- and post-transferred $\beta$-$NaYF_4$:25% Yb, 0.5% Tm UCNPs with 100 and 600 $\mu$M $(H)_6$ARAR peptides.



DOI: 10.1021/acsami.5b01446
*ACS Appl. Mater. Interfaces* 2015, 7, 11849−11856

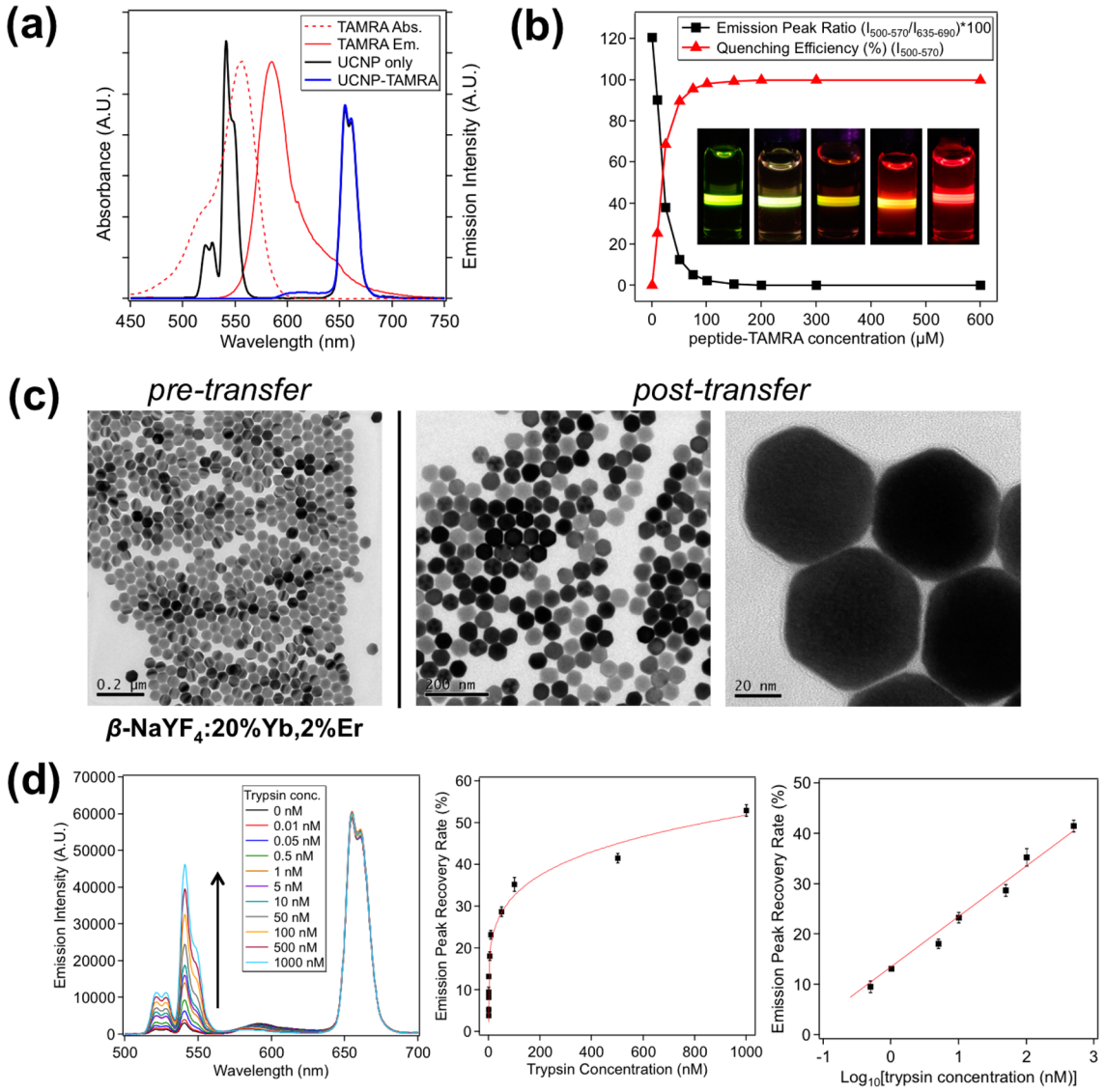


**Figure 4.** Preparation of LRET-based UCNP probes for trypsin detection. (a) Absorption (dashed red line) and emission (solid red line) spectra of TAMRA molecules and emission spectra of $\beta$-$NaYF_4$:20% Yb, 2% Er UCNPs (black line) and $\beta$-$NaYF_4$:20% Yb, 2% Er UCNP−$(H)_6$YGKAGK−TAMRA conjugates (600 $\mu$M peptides) (blue line). (b) Emission peak ratio ($I_{500-570}/I_{635-690}$) and emission peak quenching efficiency ($I_{500-570}$) of $\beta$-$NaYF_4$:20% Yb, 2% Er UCNP−$(H)_6$YGKAGK−TAMRA conjugates at different peptide concentrations (insets: luminescence photographs of UCNPs transferred with 0, 10, 25, 50, and 200 $\mu$M $(H)_6$YGKAGK−TAMRA peptides). (c) TEM images of pre- and post-transferred $\beta$-$NaYF_4$:20% Yb, 2% Er UCNPs with 150 $\mu$M $(H)_6$YGKAGK−TAMRA peptides. (d) Titration experiments for trypsin detection using $\beta$-$NaYF_4$:20% Yb, 2% Er UCNP−$(H)_6$YGKAGK−TAMRA conjugates.

while the red emission peak remains unaffected and could serve as an internal reference for ratiometric sensing (Figure 4a). To construct the probe, we used a chimeric peptide containing a polyhistidine domain, trypsin cleavage domain, and TAMRA molecule [$(H)_6$YGKAGK−TAMRA] to perform phase transfer. As expected, Er-doped UCNPs were efficiently transferred to the water layer (Figure 4c). The quenching efficiency for the green emission peak gradually increased with an elevated peptide concentration and approached nearly 100% above 150 $\mu$M peptides (Figure 4b). The overall emission color of UCNPs shifted from green to red as the green emission peak was completely quenched (insets of Figure 4b). The number of $(H)_6$YGKAGK−TAMRA peptide molecules on each UCNP (transferred with 150 $\mu$M peptides) was calculated to be 1325 (see the Supporting Information for calculation details). The as-prepared UCNPs were further aged with additional peptides and purified for trypsin detection (see the Experimental Section for details). As shown in Figure 4d, titrating UCNP probes with an increasing amount of trypsin leads to gradual recovery of the green emission peak. A wide detection range (0−1000 nM) was obtained for trypsin with high detection responsivity in the lower concentration range (0−100 nM). The detection limit is about 0.05 nM for trypsin, which is 1 order of magnitude lower than other detection methods.[3−5] It is noteworthy that the recovery rate of the green emission is in a linear relationship with the logarithm of the trypsin concentration in the range of 0.5−500 nM (Figure 4d), and thus, this method could be used for quantitative analysis of trypsin. In contrast, no recovery of the green emission peak was observed for the UCNP probes treated with BSA molecules (see Figure S5 of the Supporting Information), confirming the specificity of detection.

Next, we applied LRET-based UCNP probes for *in vivo* imaging of caspase-3 activities (Figure 5a). Because activation


DOI: 10.1021/acsami.5b01446
ACS Appl. Mater. Interfaces 2015, 7, 11849−11856

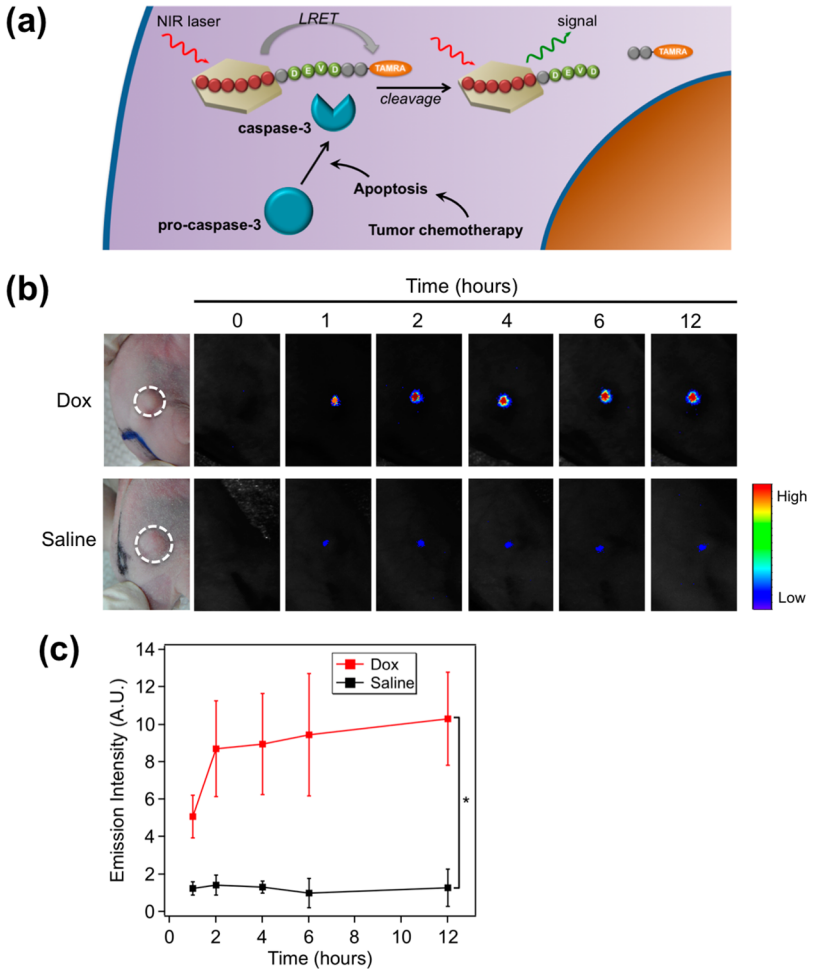


**Figure 5.** LRET-based UCNP probes for *in vivo* apoptosis imaging. (a) Schematic illustration of apoptosis-associated signal events for caspase-3 activation and subsequent cleavage of UCNP probes for apoptosis imaging. (b) *In vivo* imaging of apoptosis on xenografted mouse tumor models. UCNP probes were injected into tumors pretreated with DOX and saline; the tumor imaging was performed under 980 nm excitation; and the signal was collected between 450 and 600 nm. (c) Comparison between the average emission intensities of the tumors treated with DOX and saline ($n = 4$) (∗) $p < 0.05$ between groups indicated by brackets.

of caspase-3 is triggered by apoptotic signaling events, imaging caspase-3 activities would provide a valuable means to therapeutic efficacy evaluation and drug screening.[26] As a proof-of-concept experiment, we used our UCNP probes to measure the therapeutic efficacy of DOX on xenografted tumor mouse models. The UCNP probes were prepared via phase transfer using peptides containing a polyhistidine domain, caspase-3 cleavage domain (substate: DEVD), and TAMRA molecule [$(H)_6$GDEVDAK−TAMRA]. Cytotoxicity of these UCNP probes was evaluated using the MTT assay. Little adverse effects on cell viabilities were observed for HeLa and KB cells after incubating with UCNPs (up to 500 $\mu$g/mL) for 24 h at 37 °C (see Figure S6 of the Supporting Information), indicating that UCNP probes are suitable for *in vivo* studies. Before *in vivo* imaging, xenografted KB tumors were treated with DOX molecules twice to initiate apoptosis of tumor cells (see the Experimental Section and Figure S7 of the Supporting Information for more details). Afterward, the UCNP probes were injected into DOX-treated tumors, and the UCL signal was collected between 450 and 600 nm, with 980 nm excitation. To confirm the imaging specificity, a group of control tumors were treated with saline and the tumor imaging was performed under the same conditions. As shown in panels b and c of Figure 5, UCL was gradually activated in DOX-treated tumors but not saline-treated tumors, indicating that the UCNP probes were specific to chemotherapy treatment. It is noteworthy that, although the green emission (540 nm) is sufficient to image xenografted tumors, the longer emission peak (655 nm) would be preferred for deeper tissue imaging to afford better penetration depth. This could be realized using a fluorophore to quench selectively the longer emission peak.

## CONCLUSION

In summary, we demonstrate for the first time a facile one-step strategy to construct highly compact and stable biofunctionalized UCNPs through peptide-mediated phase transfer. This strategy is applicable for peptides with various sequences and could serve as a general strategy for peptide-functionalized UCNPs. The peptides form a compact coating layer on UCNPs to render them high stability, surface programmability, and efficient LRET. On the basis of this strategy, we show that LRET-based UCNP probes could be used for high-sensitive detection of trypsin. Moreover, we for the first time demonstrate the use of LRET-based UCNP probes for *in vivo* imaging of caspase-3 activities, which provides a useful means for *in vivo* evaluation of chemotherapy efficacy. Given the widespread applications of peptides in biosensing, biotargeting,


DOI: 10.1021/acsami.5b01446
*ACS Appl. Mater. Interfaces* 2015, 7, 11849−11856

and drug delivery, we expect that the reported peptide-mediated phase transfer strategy could be extended to construct a variety of peptide-functionalized UCNP probes for different biomedical applications.

## ■ ASSOCIATED CONTENT

### Supporting Information

UCL spectra of phase-transferred UCNPs, stained TEM image of peptide-coated UCNPs, colloidal stability of peptide-coated UCNPs, cytotoxicity of UCNPs, tumor growth curves, and calculations of the number of peptides on each UCNP (PDF). The Supporting Information is available free of charge on the ACS Publications website at DOI: 10.1021/acsami.5b01446.

## ■ AUTHOR INFORMATION

### Corresponding Author

*E-mail: nan.ma@suda.edu.cn.

### Notes

The authors declare no competing financial interest.

## ■ ACKNOWLEDGMENTS

This work was supported in part by the National Natural Science Foundation of China (NSFC) (21175147, 91313302, and 21475093), the National High-Tech Research and Development Program (2014AA020518), the 1000-Young Talents Plan, PSTI of Suzhou (SZS201207), PAPD, and startup funds from Soochow University.

## ■ REFERENCES

(1) Razgulin, A.; Ma, N.; Rao, J. Strategies for *in vivo* imaging of enzyme activity: An overview and recent advances. *Chem. Soc. Rev.* **2011**, *40*, 4186−4216.

(2) Vickers, C. J.; González-Páez, G. E.; Wolan, D. W. Selective detection and inhibition of active caspase-3 in cells with optimized peptides. *J. Am. Chem. Soc.* **2013**, *135*, 12869−12876.

(3) He, X.; Ma, X.; Biomimetic, N. Synthesis of fluorogenic quantum dots for ultrasensitive label-free detection of protease activities. *Small* **2013**, *9*, 2527−2531.

(4) Wang, Y.; Zhang, Y.; Liu, B. Conjugated polyelectrolyte based fluorescence turn-on assay for real-time monitoring of protease activity. *Anal. Chem.* **2010**, *82*, 8604−8610.

(5) Seo, S.; Kim, J.; Jang, G.; Kim, D.; Lee, T. S. Aggregation−deaggregation-triggered, tunable fluorescence of an assay ensemble composed of anionic conjugated polymer and polypeptides by enzymatic catalysis of trypsin. *ACS Appl. Mater. Interfaces* **2014**, *6*, 918−924.

(6) Li, J.; Li, X.; Shi, X.; He, X.; Wei, W.; Ma, N.; Chen, H. Highly sensitive detection of caspase-3 activities via a nonconjugated gold nanoparticle-quantum dot pair mediated by an inner-filter effect. *ACS Appl. Mater. Interfaces* **2013**, *5*, 9798−9802.

(7) Wang, F.; Han, Y.; Lim, C. S.; Lu, Y.; Wang, J.; Xu, J.; Chen, H.; Zhang, C.; Hong, M.; Liu, X. Simultaneous phase and size control of upconversion nanocrystals through lanthanide doping. *Nature* **2010**, *463*, 1061−1065.

(8) Haase, M.; Schafer, H. Upconverting nanoparticles. *Angew. Chem., Int. Ed.* **2011**, *50*, 5808−5829.

(9) Zhou, J.; Liu, Z.; Li, F. Upconversion nanophosphors for small-animal imaging. *Chem. Soc. Rev.* **2012**, *41*, 1323−1349.

(10) Chen, G.; Qiu, H.; Prasad, P. N.; Chen, X. Upconversion nanoparticles: Design, nanochemistry, and applications in theranostics. *Chem. Rev.* **2014**, *114*, 5161−5214.

(11) Chen, G. Y.; Ohulchanskyy, T. Y.; Law, W. C.; Agren, H.; Prasad, P. N. Monodisperse $NaYbF_4$:$Tm^{3+}$/$NaGdF_4$ core/shell nanocrystals with near-infrared to near-infrared upconversion photoluminescence and magnetic resonance properties. *Nanoscale* **2011**, *3*, 2003−2008.

(12) Li, Z. Q.; Zhang, Y. Monodisperse silica-coated polyvinylpyrrolidone/$NaYF_4$ nanocrystals with multicolor upconversion fluorescence emission. *Angew. Chem., Int. Ed.* **2006**, *45*, 7732−7735.

(13) Chen, Z.; Chen, H.; Hu, H.; Yu, M.; Li, F.; Zhang, Q.; Zhou, Z.; Yi, T.; Huang, C. Versatile synthesis strategy for carboxylic acid-functionalized upconverting nanophosphors as biological labels. *J. Am. Chem. Soc.* **2008**, *130*, 3023−3029.

(14) Jiang, G. C.; Pichaandi, J.; Johnson, N. J. J.; Burke, R. D.; van Veggel, F. C. J. M. An effective polymer cross-linking strategy to obtain stable dispersions of upconverting $NaYF_4$ nanoparticles in buffers and biological growth media for biolabeling applications. *Langmuir* **2012**, *28*, 3239−3247.

(15) Zhang, P.; Rogelj, S.; Nguyen, K.; Wheeler, D. Design of a highly sensitive and specific nucleotide sensor based on photon upconverting particles. *J. Am. Chem. Soc.* **2006**, *128*, 12410−12411.

(16) Li, L.-L.; Zhang, R.; Yin, L.; Zheng, K.; Qin, W.; Selvin, P. R.; Lu, Y. Biomimetic surface engineering of lanthanide-doped upconversion nanoparticles as versatile bioprobes. *Angew. Chem., Int. Ed.* **2012**, *51*, 6121−6125.

(17) Boeneman, K.; Mei, B. C.; Dennis, A. M.; Bao, G.; Deschamps, J. R.; Mattoussi, H.; Medintz, I. L. Sensing caspase-3 activity with quantum dot-fluorescent protein assemblies. *J. Am. Chem. Soc.* **2009**, *131*, 3828−3829.

(18) Dechantsreiter, M. A.; Planker, E.; Matha, B.; Lohof, E.; Holzemann, G.; Jonczyk, A.; Goodman, S. L.; Kessler, H. N-Methylated cyclic RGD peptides as highly active and selective $\alpha_V\beta_3$ integrin antagonists. *J. Med. Chem.* **1999**, *42*, 3033−3040.

(19) Stewart, K. M.; Horton, K. L.; Kelley, S. O. Cell-penetrating peptides as delivery vehicles for biology and medicine. *Org. Biomol. Chem.* **2008**, *6*, 2242.

(20) Hoffmann, A.; Roeder, R. G. Purification of His-tagged proteins in non-denaturing conditions suggests a convenient method for protein interaction studies. *Nucleic Acids Res.* **1991**, *19*, 6337−6338.

(21) Medintz, I. L.; Clapp, A. R.; Mattoussi, H.; Goldman, E. R.; Fisher, B.; Mauro, J. M. Self-assembled nanoscale biosensors based on quantum dot FRET donors. *Nat. Mater.* **2003**, *2*, 630−638.

(22) Ma, N.; Sargent, E. H.; Kelley, S. O. Biotemplated nanostructures: Directed assembly of electronic and optical materials using nanoscale complementarity. *J. Mater. Chem.* **2008**, *18*, 954−964.

(23) Zhao, J.; Jin, D.; Schartner, E. P.; Lu, Y.; Liu, Y.; Zvyagin, A. V.; Zhang, L.; Dawes, J. M.; Xi, P.; Piper, J. A.; Goldys, E. M.; Monro, T. M. Single-nanocrystal sensitivity achieved by enhanced upconversion luminescence. *Nat. Nanotechnol.* **2013**, *8*, 729−734.

(24) Soreide, K.; Janssen, E. A.; Korner, H.; Baak, J. P. A. Trypsin in colorectal cancer: Molecular biological mechanisms of proliferation, invasion, and metastasis. *J. Pathol.* **2006**, *209*, 147−156.

(25) Wang, F.; Liu, X. Upconversion multicolor fine-tuning: Visible to near-infrared emission from lanthanide-doped $NaYF_4$ nanoparticles. *J. Am. Chem. Soc.* **2008**, *130*, 5642−5643.

(26) Ye, D.; Shuhendler, A. J.; Cui, L.; Tong, L.; Tee, S. S.; Tikhomirov, G.; Felsher, D. W.; Rao, J. Bioorthogonal cyclization-mediated *in situ* self-assembly of small-molecule probes for imaging caspase activity *in vivo*. *Nat. Chem.* **2014**, *6*, 519−526.



DOI: 10.1021/acsami.5b01446
*ACS Appl. Mater. Interfaces* 2015, 7, 11849−11856